CrossMark

ORIGINAL PAPER

Formation Factors of the Surface Layer Generated from Serpentine as Lubricant Additive and Composite Reinforcement

Junwei Wu[1] · Xiao Wang[1] · Luhai Zhou[1] · Xicheng Wei[1] · Wurong Wang[1]

Abstract Serpentine is usually added into oil for tribological applications. To explore the performance and mechanism of serpentine, three different kinds of pins were tested under lubricated/dry sliding conditions. The result shows that a surface layer with an excellent anti-friction property was formed on the surface of worn steel. The binding ability between the matrix elements in the wear-induced transition zone and the unsaturated bonds released by serpentine is the key factor to form the anti-friction surface layer. Meanwhile, the hardness of the pairing material and frictional contact time determine the thickness and surface roughness of the anti-friction surface layer. In all, this work is hoped to be helpful in designing and researching a new industrial anti-friction material which can be used for dry sliding conditions.

1 Introduction

Serpentine is a natural hydrous phyllosilicate mineral, and its chemical formula is $Mg_2Si_2O_5(OH)_4$. Serpentine has been applied in many fields worldwide. For example, it can be used for synthesizing silicon carbide [1] and for storing the carbon dioxide in the atmosphere [2, 3]. In addition, Zhang and Sugiyama [4] extracted magnesium and silicon from serpentine by mechanochemical treatment.

Serpentine powder as additive in oil for tribological applications has also been widely investigated. It is able to form a self-repairing protective layer on worn ferrous alloy surface [5], which decreases the friction coefficient and prevents substrate from being damaged [6, 7]. Physical model [8] and phenomenological model [9] were developed to discuss the possible formation mechanism of the surface-coated layer. According to Wang [10], it is believed that the physical and mechanical effects, involving adhering and spreading on the worn surface, are the leads to the formation of the self-repairing protective layer. In addition, mechanochemical and thermochemical reaction also plays certain significant role on its formation [11].

However, the essence and physical nature of the formation of the self-repairing surface layer have so far not been sufficiently clarified [12]. Former works have mainly conjectured the formation mechanisms of surface layer between ferrous friction pairs with serpentine doped in the lubricant. Therefore, more efforts are required to further explore the mechanisms. In our experiment, nonferrous friction pairs were introduced in order to better understand the formation process of surface layer induced by serpentine during friction. Cu–40Zn brass was rubbed against GCr15 steel under the lubrication of serpentine-contained oil. In contrast, Cu–40Zn–serpentine composite was fabricated to rub against the GCr15 steel without lubrication. It is hoped to prove the factors of forming the self-repairing surface layer and in designing a new industrial anti-friction composite used for dry sliding conditions, like piston rings.

✉ Xicheng Wei
  wxc1028@staff.shu.edu.cn

1 School of Materials Science and Engineering, Shanghai University, Shanghai 200072, People's Republic of China

2 Experimental Details

2.1 Materials

The experimental lubricant oil in the present work was a mixture of 0.38 g serpentine powder and 75.62 g KTL32 turbine oil which was suitable for bearing (the mass ratio of 1:199) [12]. Cu–40%Zn brass and brass–1% serpentine composite were fabricated by the method of powder metallurgy. The producer or supplier and the characteristics of the individual powders are given in Table 1.

Figure 1 shows the X-ray diffraction pattern and SEM image of the serpentine powders. The diffraction peaks of $d = 0.7282$, 0.3617, 0.2765, and 0.2519 nm can be indexed to those of antigorite. The powder size is mostly in the range of 0.1–1 μm.

Powder metallurgy method was presented as follows: The powders were mixed in a high-energy planetary ball mill for 3 h [13], with the weight ratio of ball to powder of 2:1 [14] and the milling speed of 350 rpm [15]. After that, the powder mixtures were cold pressed uniaxially into cylindrical pre-forms at the pressure of 500 MPa [16]. Sintering process was carried out using a YFK-60X400 pipe electric furnace. The compacts were sintered at the temperature of 870 ° C for 3 h in the protective atmosphere and followed by furnace cool-ing. The protective atmosphere was mixed with 99.9% purity nitrogen and hydrogen in the ratio of 1:1 in order to prevent the composite being oxidized.

2.2 Wear Test and Materials

Sliding friction test was performed on a MM-W1 three pin-on-disk apparatus in a laboratory environment. The schematic diagrams and dimensions of pin and disk are shown in Fig. 2. The disk was rotated, and the pin was fixed during test with the turning radius of 13 mm. Before and after the test, specimens were cleaned with petroleum ether and absolute ethyl alcohol by ultrasonic cleaner for 15 min by ultrasonic cleaner. The average friction coefficient was recorded by an attached computer sensor. The selected normal load was 80 N, the sliding speed was 0.73 m/s, and test duration was 80 min.

Three experiment conditions were designed, as shown in Table 2. To compare the experimental effect of serpentine,
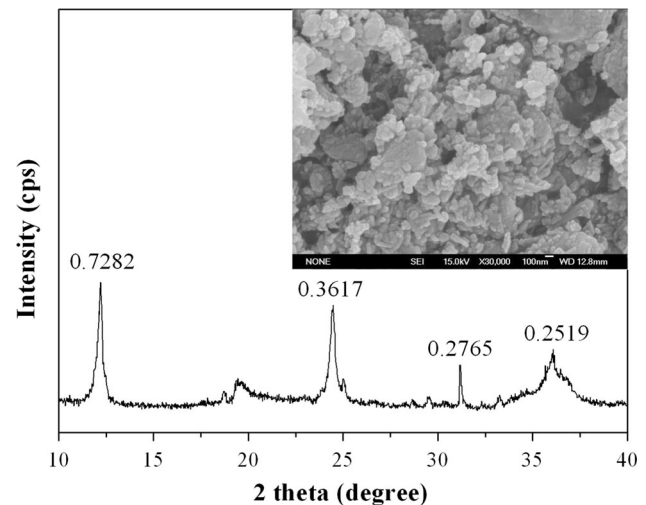

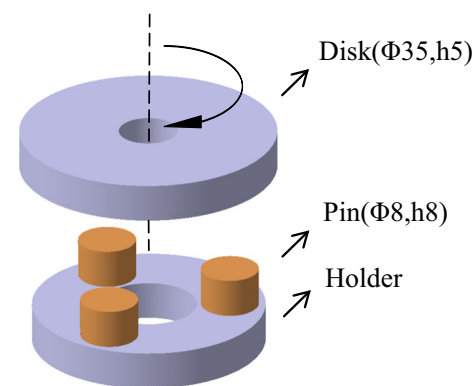Fig. 1 XRD pattern and SEM image of serpentine powders

Fig. 2 Schematic diagrams and dimensions of pin and disk

three comparative tests were also made. The sliding fric-tion test was carried out for three times, and their average was used. The hardness of GCr15 steel, Cu–40Zn brass, and Cu–40Zn–serpentine composite was about 60.3, 22.1, and 20.8 HRC, respectively. The surface roughness of the disk and pin specimens was Ra 0.05–0.1 μm.

2.3 Characterization Method

The decomposition temperature of serpentine powders was investigated by a STA449F3 thermal analyzer which

Table 1 Producers/suppliers and characteristics of examined powders

Powder	Producer/supplier	Powder characteristics
Cu	Zhejiang Jililai New Material Co., Ltd.	Mesh ≤100
Zn		Water atomized
		Irregular shape particles
Serpentine	Baosteel, China.	Size 0.1–1 μm
		Density 2.7×10^3 kg/m³ at 25 ° C

Table 2 Experiment conditions of three tribo-pairs

Tribo-pair	#1		#2		#3	
	Disk	Pin	Disk	Pin	Disk	Pin
Materials	GCr15	GCr15	GCr15	Brass	GCr15	Composite
Lubrication condition	Lubricant oil with serpentine		Lubricant oil with serpentine		Dry sliding	
Comparative test	Lubricant oil without serpentine		Lubricant oil without serpentine		Pin without serpentine	

allows simultaneous differential scanning calorimetry (DSC) and thermogravimetry (TG). The range of scanning temperature was chosen from room temperature to 1000 ° C, while the heating rate was at 10 ° C/min. The protection gas was nitrogen.

The Rockwell C hardness tester was used to measure hardness of specimens under a load of 600 N corresponding to GB/T 230.2-2012, and an average of five points was used for each sample. The surface roughness of the sample was conducted out on a SE500 roughness tester.

A HITACHI S-570 scanning electronic microscope (SEM) equipped with an oxford energy-dispersive spectroscopy (EDS) was used to observe the morphologies of cross section of the samples. A HITACHI SU-1500 SEM equipped with an oxford EDS was used to observe the morphologies of the worn surface of the samples.

3 Results

3.1 Cross-Section Morphologies

Figure 3 presents the cross-section morphologies of the worn disks. It can be seen that the disk was covered with a surface layer that was different from the matrix. #1 disk had thinnest surface layer, with the thickness of about 1.0 μm, while #3 disk had the roughest but thickest one, with the thickness of about 2.0 μm. The surface layer of #2 disk was about 1.9 μm thick and relatively rougher than that of #1 disk. Meanwhile, the black transition zone between the surface layer and the matrix appeared. The width of transition zones of the disks were about 1.5, 6, and 3 μm, respectively.

The cross-section morphologies of the pins are shown in Fig. 4. The evenly distributed surface layer on #1 pin was about 2 μm thick in average. Compared with the surface layers of the disks, it seems to be more compact and better adhered with the matrix. However, the brass pin and the composite pin had almost no surface layer covered on them.
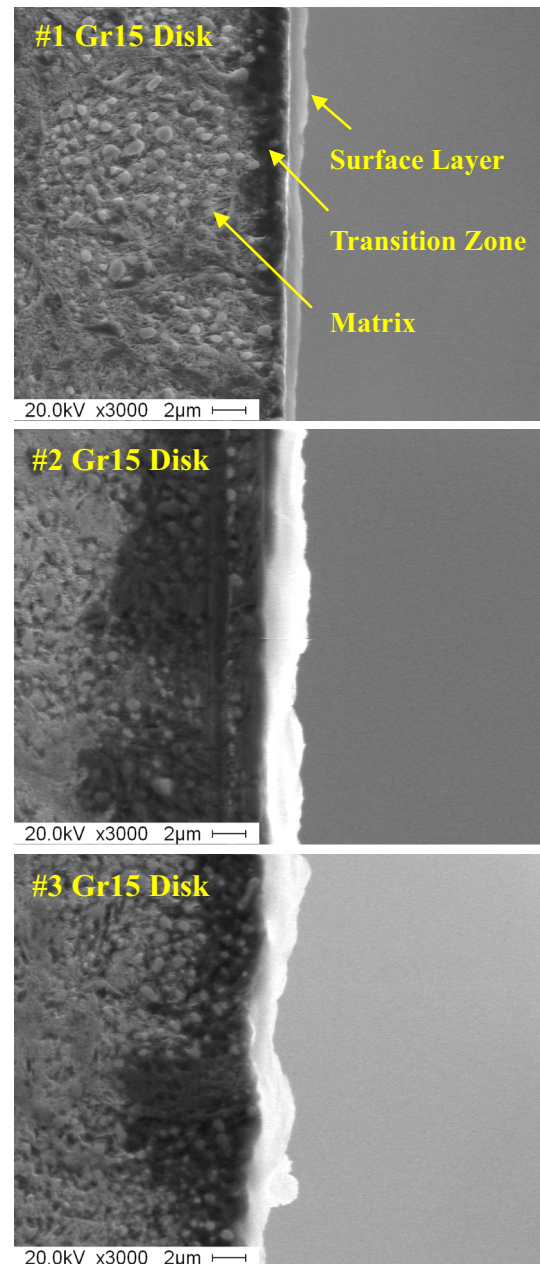
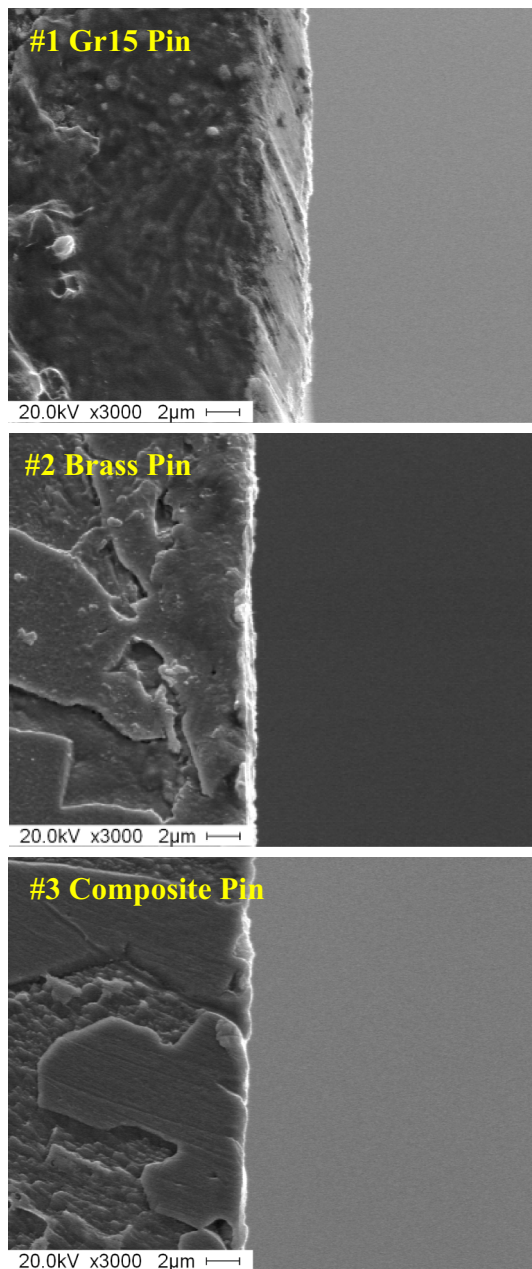**Fig. 3** Cross-section morphologies of the worn disks

Fig. 4 Cross-section morphologies of the pins

3.2 Worn Surface Morphologies

Figure 5 is the worn surface morphologies of the disks. Pitting spalling morphology concentrated in the furrows of #1 disk surface. EDS spectra of Fig. 5a indicate the presence of Mg and Si elements at the pitting spalling spots, which should be the source of serpentine. With the morphologies of cross section in Fig. 3a, it can be conjectured that the surface layer was generated from serpentine on #1 disk.

The surface layer of #2 disk (Fig. 5b) was relatively rougher than that of #1 disk in Fig. 5a, which corresponds with the cross-sectional results shown in Fig. 3. Meanwhile, higher contents of Mg, Si elements and lower contents of Fe element in the EDS results signified that the elements of serpentine composition exist in a certain micrometer from the surface, proving the thicker surface layer of #2 disk than #1 disk.

Moreover, the serpentine powder can be delivered uniformly to the friction surface with the lubricant oil. Nevertheless, without lubrication, the new serpentine powders would not appear until the surface of the composite is rubbed. Therefore, #3 disk was found to gain a novel worn surface on worn surface. The serpentine particle was deeply embedded in the furrows and scratches of the matrix and was absorbed on the worn surface. A surface layer was gradually formed around the embedded serpentine powder, covering the furrows and grooves partially with the friction time prolonged. The region along the surface layer became smoother, as can be seen in Fig. 5c when comparing with the typical abrasive wear morphology beside the serpentine particle.

3.3 Friction Coefficient

Figure 6 shows the friction coefficient and wear loss comparison of three tribo-pairs. With the lubrication of serpentine doped oil, #1 tribo-pair had the lowest friction coefficient of 0.016, while the friction coefficient of #2 tribo-pair was 0.027. In comparison, both friction coefficients of #1 and #2 tribo-pair were increased and came to 0.030 and 0.042, respectively, when lubricated by the oil without serpentine. Under the dry sliding condition, #3 tribo-pair possessed a low average friction coefficient of 0.141, compared with 0.175 for #3 tribo-pair without serpentine. An anti-friction effect can be concluded when serpentine was being used in the forms of lubricant additive and composite reinforcement.

The friction coefficient of #1 tribo-pair gradually decreased to 0.007 and remained stable, while its datum specimen gradually increased to 0.042. Similarly, the friction coefficient of #2 tribo-pair remained at 0.029, while its datum specimen gradually kept stable at 0.048. Also, the friction coefficient of #3 tribo-pair stayed around at 0.177, while its datum specimen gradually stayed around at 0.187. As a result, both the pin and the disk of #1 tribo-pair were covered with surface layer, decreasing the friction coefficient effectively with the friction time prolonged. The anti-friction effect was weakened since only the disk was covered with the surface layer in #2 tribo-pair. Even limited region of #3 disk was covered with the surface layer, the friction coefficient was decreased. It is proved that the surface layer has an excellent property of anti-friction.
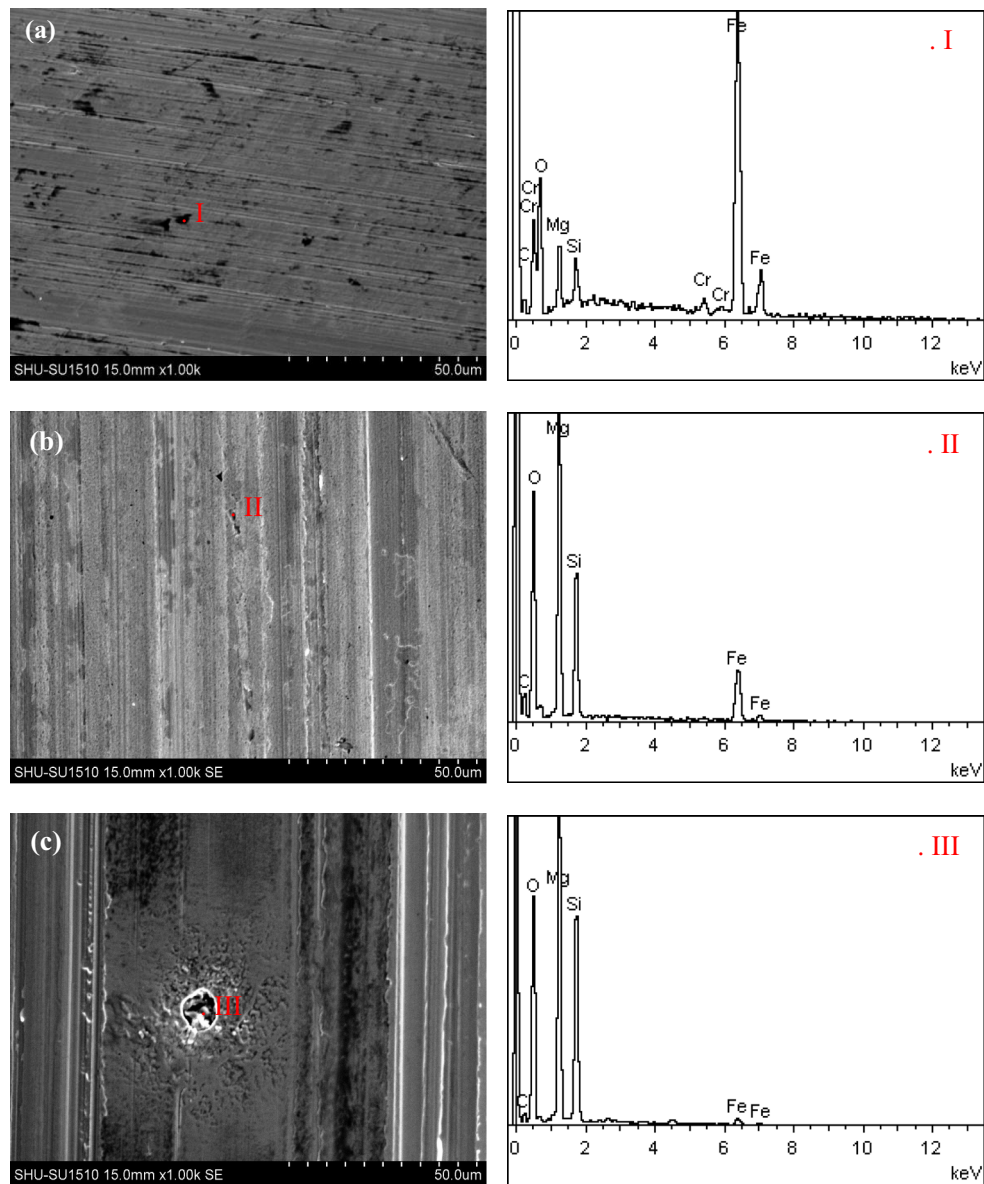
Fig. 5 Worn surface morphologies and corresponding EDS spectrum of the disks

Furthermore, the wear losses of all the three disks were decreased and #3 disk even showed a negative wear loss with the formation of the surface layer generated from serpentine. Conjectured with Fig. 3, the mass rising rate induced by the formation of the surface layer could compensate or even exceed the wear loss rate caused by the friction and wear.

4 Discussions

Jin et al. [5] found that under the condition of multibody friction, serpentine as lubricant additive would form an auto-reconditioning protective layer on worn ferrous surface. Jia et al. [17] presented a PTFE/serpentine composite and found the hybrid transfer film generated on the surface of mating pair was likely responsible for the lower wear rate. The present work used three tribo-pairs with the same experiment condition, and several factors can be confirmed to affect the formation of the surface layer generated from serpentine.

4.1 Hardness of the Pairing Material

One factor is the hardness of the pairing material. Yu et al. [9] found that a tribofilm was formed on the worn surface under the lubrication of oil with serpentine, making the surface hardness higher than its matrix 1045 steel (29–31
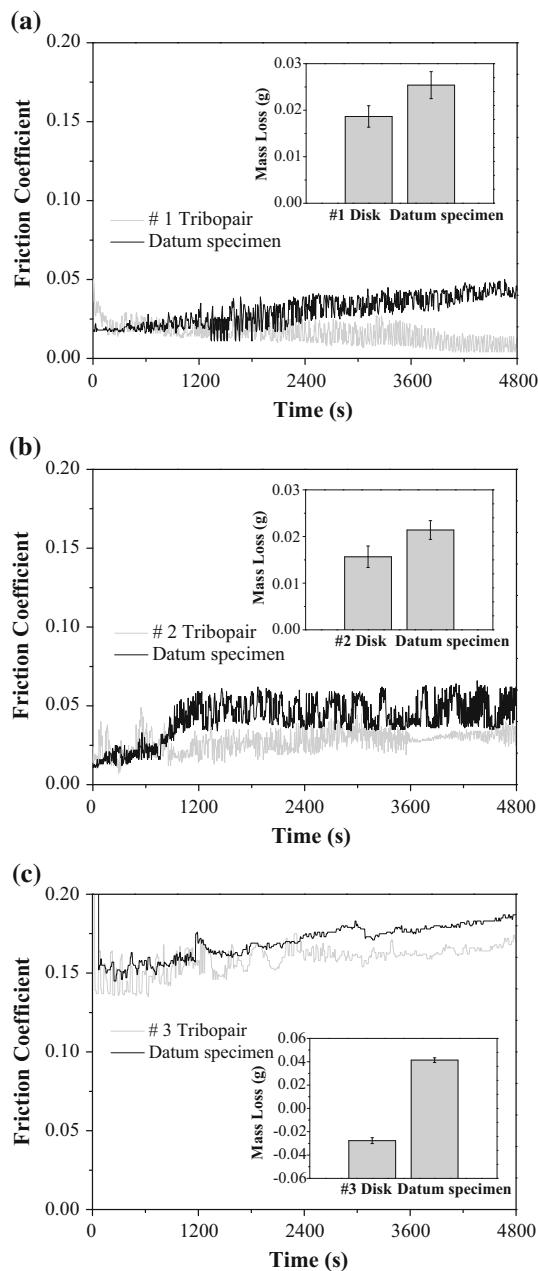
Fig. 6 Friction coefficient and wear loss comparison of **a** #1; **b** #2; **c** #3 tribo-pair

HRC). In the present work, it can be found that the surface layer of the disks became thicker with the decreasing of the pin hardness. In addition, the surface roughness of the surface layer increased at the same time. It is known that friction will deform the contact surface, the deformation of the asperities and the contact stress will affect each other as illustrated in Fig. 7a. During the sliding friction process, the pin would deform the disk surface strongly, generating high pressures. After lubricated by the serpentine-contained oil, Yu et al. [11] found that the ratio of hardness to modulus of friction surface was observably increased,

improving the wear resistance of worn surface. So the harder pin would be more easily to deform the surface layer, making it smoother and thinner. If the hardness of pin was low, the new surface layer could be accumulated on the former layer before it was rubbed off. As a result, the surface layer became thick and rough.

Meanwhile, the black transition zone between the surface layer and the matrix was appeared, which can be seemed as a deformation layer (Fig. 3). Wang et al. [18] investigated the sliding friction-induced deformation layer on 20CrMnTi, and the formation of ultrafine grain and even nanocrystalline was the result of it. When ductile materials such as copper [19], aluminum [20], and austenitic stainless steels [21] are sliding against other materials, nanostructure in the worn surface layer is usually formed. In the present work, a similar wear-induced transition zone was formed with the illustration shown in Fig. 7b. The maximum wear loss of disk frictional sliding against the hardest pin would easily bring a new disk surface, making the transition zone of #1 disk shallowest for all the three, as shown in Figs. 3 and 6. It should be noted that the activity of Fe atoms in the transition zone would be highly enhanced, so the surface layer would be more likely to be formed over the deep transition zone and become thicker.

4.2 Frictional Contact Time

Another factor should be the frictional contact time of the matrix. Compared with the surface layer of the GCr15 disk, the one of GCr15 pin was thicker, more compact and better adhered with the matrix, as shown in Figs. 3 and 4. During the friction contact process, the disk was rotated and intermittently contacted while the pin was rubbed all the time. GCr15 pin experienced a four times longer frictional contact time, as can be calculated by surface area ratio of disk and pins shown in Fig. 2. Longer frictional contact time makes the friction temperature higher and more reaction to maintain. Kalin [23] suggested the highest flash temperatures in the contacts were above $1100\ ^\circ C$ in a mineral base-oil-lubricated condition. To analyze the tribological decomposition behavior of serpentine at high temperature, the DSC–TG curves of the serpentine powder are made in Fig. 8. It can be seen that the DSC curve had a large endothermic peak at $115\ ^\circ C$ and the corresponding TG curve started to decline. It was caused by dehydrating absorbed water from the serpentine powder [24, 25]. The mass percent of adsorbed water accounted for 1% of serpentine weight. Another deep and wide endothermic peak appeared at $668\ ^\circ C$, where the structure of serpentine changed and new phases generated. As shown in the TG curve, a substantial thermal weight loss of the serpentine powder occurred, and it is believed that the endothermic peak

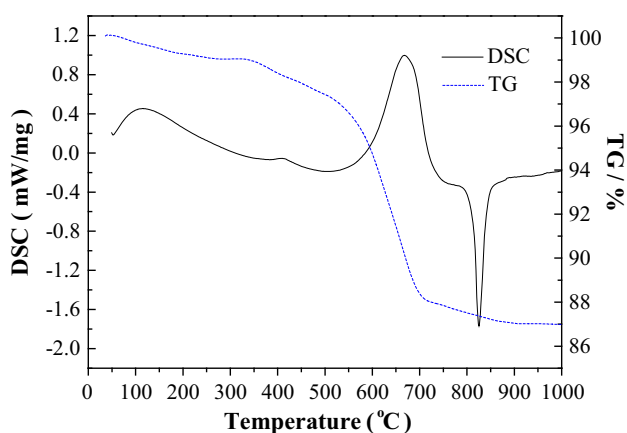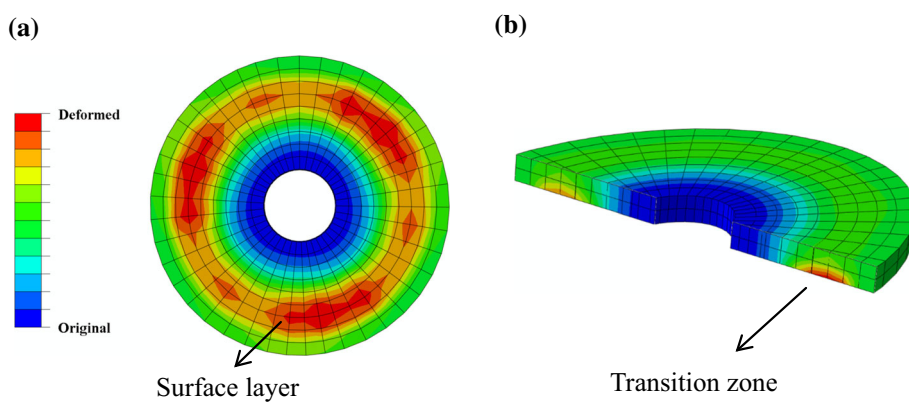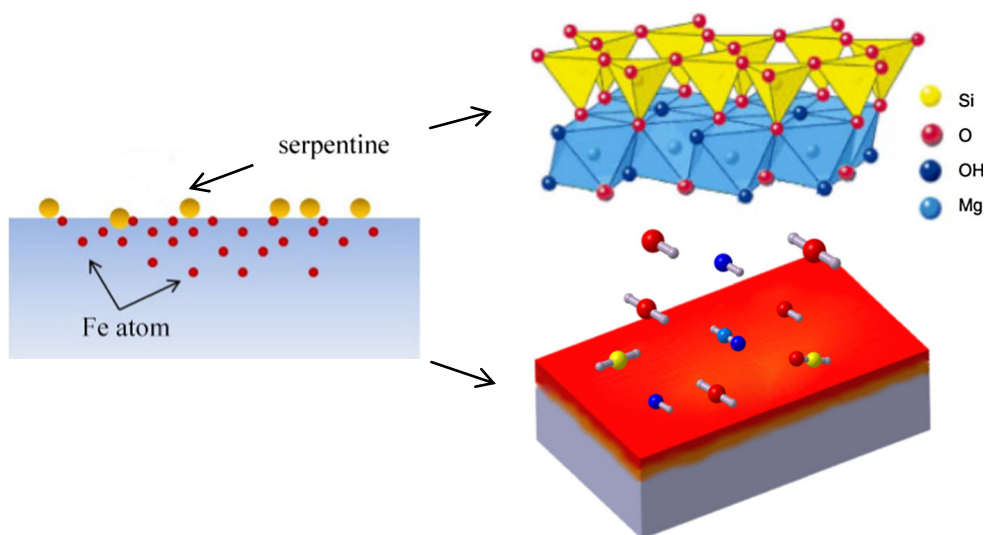**Fig. 7** Schematic diagrams of **a** surface layer; **b** transition zone [22]

(a)

Deformed

Original

Surface layer

(b)

Transition zone

Fig. 8 DSC and TG curves of the serpentine powder

transformed [24–27], releasing active –O, –O–, –Si–, –Si–O, –OH, and –Mg–OH atoms.

Figure 9 illustrates the schematic diagram of in situ formation of surface layer. According to Wang et al. [28], the atomic diffusion phenomenon is considered to be the result of joint action of temperature rise on the contact surfaces and grain refinements in the sliding friction-induced deformation layer. Moreover, Lai et al. reported that the specific surface area of the original serpentine particles can be increased by more than 20 times after heated at 550 °C. The serpentine particles acted as abrasives, making the friction coefficient fluctuated at first (Fig. 6). After continued friction, the serpentine powders were filled into the furrows and scratches of the matrix (Fig. 5). Under the effect of friction heat, the adsorptive capacity of serpentine could be improved. Active –O, –O–, –Si–, –Si–O, –OH, and –Mg–OH unsaturated bonds released by serpentine would react with the highly activated Fe atoms in the transition zone to form the Fe_2O_3 and FeO, as detected by the EDS of Fig. 5. In addition, with the break of the

corresponded to a dehydroxylation reaction [25, 26]. When the temperature reached 826 °C, a strong and sharp exothermic peak appeared. The structure of serpentine at this peak was completely destroyed and

Fig. 9 Schematic diagram of in situ formation of surface layer

serpentine

Fe atom

Si

O

OH

Mg

–O–Si–O– and –OH–Mg–O of the embedded serpentine, the Fe ion of the transition zone would replace Si and Mg to form –O–Fe–O and –OH–Fe–O. With the interaction of serpentine and the transition zone, an in situ surface layer was generated.

4.3 Binding Ability Between Serpentine and Matrix

As illustrated in Fig. 9, the matrix atoms/ions have to bind with the unsaturated bonds of –O, –O–, –Si–, –Si–O, –OH, and –Mg–OH. Similarly, former results [9–13] also showed that the surface layer was mainly composed of oxides. The brass pin and the composite pin, other than GCr15 pin, had almost no surface layer covered on them. So the binding ability should be taken into consideration to analyze the formation of the surface layer.

In this work, the pin experienced the large friction pressure and high temperature during the sliding process, and thus, the transition zone (Fig. 3) was induced by friction and wear where the activities of pin elements were highly activated. It should be noted that the GCr15 pin mainly consisted of Fe, and the brass pin and the composite pin mainly consisted of Cu. Yua et al. [29] reported that O binding energy of Fe (2.72 eV) is lower than that of Cu (3.41 eV), and OH binding energy of Fe (1.63 eV) is lower than that of Cu (2.06 eV). So Fe would be more likely to react with the unsaturated bonds released by serpentine. However, Cu of the brass pin and the composite pin was hard to be bound, so the surface layer was difficult to be formed on the brass pin or the composite pin surface. Therefore, the binding ability can be considered to be the key factor to form an in situ surface layer.

4.4 Design of a New Anti-friction Machine Parts

In the condition of #1 and #2 tribo-pairs, large amounts of serpentine were doped in the lubricant oil. When the absorbed serpentine on the contact surface is consumed, the serpentine in the oil can be transferred to the contact surface immediately. As a result, the surface layer can be formed directly after it is destroyed, showing the self-repairing effect. However, in the condition of #3 tribo-pair, the new serpentine powders will not appear until the surface of the composite is rubbed. Compared with the other tribo-pairs in Fig. 5c, fewer serpentine particles would appear on #3 tribo-pair worn surface. But once they are embedded on the surface, they will be compressed and sheared for a longer time. So they can react with the disk matrix adequately, making the surface layer thicker.

And it should be noted that the friction coefficient of the brass–serpentine composite under the dry sliding friction was obviously lower than that of the traditional brass. An anti-friction layer can be formed on its pairing steel and cover the worn surface, compensating the wear loss and showing the self-repairing function (Figs. 5, 6). Therefore, the serpentine can be taken as an effective anti-friction reinforcement. Machine parts like piston ring and bearing bush can thus be replaced by serpentine-reinforced composites.

5 Conclusions

The sliding friction test of three different kinds of tribo-pairs were carried out and the formation mechanism of self-repairing surface layer was discussed in detail, following main conclusions have been drawn on the basis of experimental results.

1. A surface layer with an excellent anti-friction property was formed on the worn steel surface. Softer pairing material makes the surface layer thicker and rougher. Similarly, longer frictional contact time makes the surface layer thicker, more compact, and better adhered with the matrix.
2. The compressive stress and the friction heat contribute to the formation of the surface layer, while the binding ability between the matrix elements in the wear-induced transition zone and the unsaturated bonds released by serpentine determines whether or not the surface layer can be formed.
3. Serpentine-reinforced composite has a combined feature of anti-friction and self-repairing, making it a promising industrial anti-friction material used for dry sliding conditions, like piston rings.

References

1. Cheng, T.W., Hsu, C.W.: A study of silicon carbide synthesis from waste serpentine. Chemosphere **64**, 510–514 (2006)
2. Schulze, R.K., Hill, M.A., Field, R.D., Papin, P.A., Hanrahan, R.J., Byler, D.D.: Characterization of carbonated serpentine using XPS and TEM. Energy Convers. Manag. **45**, 3169–3179 (2004)
3. Farhanga, F., Olivera, T.K., Raysonb, M., Brentb, G., Stockenhubera, M., Kennedy, E.: Experimental study on the precipitation of magnesite from thermally activated serpentine for CO_2 sequestration. Chem. Eng. J. **1**, 439–449 (2016)
4. Zhang, Q.W., Sugiyama, K., Saito, F.: Enhancement of acid extraction of magnesium and silicon from serpentine by mechanochemical treatment. Hydrometallurgy **45**, 323–331 (1997)

5. Jin, Y.S., Li, S.H., Zhang, Z.Y., Yang, H., Wang, F.: In situ mechanochemical reconditioning of worn ferrous surfaces. Tribol. Int. **37**, 561–567 (2004)

6. Higgs III, C.F., Wornyoh, E.Y.A.: An in situ mechanism for self-replenishing powder transfer films: experiment sand modeling. Wear **264**, 131–138 (2008)

7. Zhao, F.Y., Kasrai, M., Sham, T.K., Bai, Z.M.: Characterization of tribofilms generated from serpentine and commercial oil using X-ray absorption spectroscopy. Tribol. Lett. **50**, 287–297 (2013)

8. Pogodaev, L.I., Buynaovskii, I.A., Kryukov, E.Y.: The mechanism of interaction between natural laminar hydrosilicates and friction surfaces. J. Mach. Manuf. Reliab. **38**, 476–484 (2009)

9. Yu, H.L., Xu, Y., Shi, P.J., Wang, H.M., Wei, M., Zhao, K.K., Xu, B.S.: Microstructure, mechanical properties and tribological behavior of tribofilm generated from natural serpentine mineral powders as lubricant additive. Wear **297**, 802–810 (2013)

10. Wang, F.: Research on microstructure of the auto-restoration layer of worn surface of metals. Mater. Sci. Eng. A **399**, 271–275 (2005)

11. Yu, H.L., Xu, Y., Shi, P.J.: Tribological behaviors of surfaced-coated serpentine ultrafine powders as lubricant additive. Tribol. Int. **43**, 667–675 (2010)

12. Zhang, B.S., Xu, Y., Gao, F., Shi, P.J., Xu, B.S., Wu, Y.X.: Sliding friction and wear behaviors of surface-coated natural serpentine mineral powders as lubricant additive. Appl. Surf. Sci. **257**, 2540–2549 (2011)

13. Wang, X., Wu, J.W., Wei, X.C., Liu, R.D., Cao, Q.: The effect of serpentine additive on energy-saving and auto-reconditioning surface layer formation. Ind. Lubr. Tribol. **69**, 158–165 (2017)

14. Jin, K.J., Qiao, Z.H., Zhu, S.Y., Cheng, J., Yin, B., Yang, J.: Synthesis effects of Cr and Ag on the tribological properties of Cu–9Al–5Ni–4Fe–Mn bronze under seawater condition. Tribol. Int. **101**, 69–80 (2016)

15. Zhang, B.S., Xu, B.S., Xu, Y., Gao, F., Shi, P.J., Wu, Y.X.: Cu nanoparticles effect on the tribological properties of hydrosilicate powders as lubricant additive for steel–steel contacts. Tribol. Int. **44**, 866–878 (2011)

16. Almomani, M.A., Tayfour, W.R., Nimrat, M.H.: Effect of silicon carbide addition on the corrosion behavior of powder metallurgy Cu–30Zn brass in a 3.5 wt% NaCl solution. J. Alloys Compd. **679**, 104–114 (2016)

17. Jia, Z.N., Yang, Y.L., Chen, J.J., Yu, X.J.: Influence of serpentine content on tribological behaviors of PTFE/serpentine composite under dry sliding condition. Wear **268**, 996–1001 (2010)

18. Wang, X., Wei, X.C., Hong, X.L., Yang, J.Y., Wang, W.R.: Formation of sliding friction-induced deformation layer with nanocrystalline structure in T10 steel against 20CrMnTi steel. Appl. Surf. Sci. **280**, 381–387 (2013)

19. Singh, J.B., Wen, J.G., Bellon, P.: Plastic strain-induced grain refinement in the nanometer scale in a Mg alloy. Acta Mater. **56**, 3053–3064 (2008)

20. Meng-Burany, X., Perry, T.A., Sachdev, A.K., Alpas, A.T.: Subsurface sliding wear damage characterization in Al–Si alloys using focused ion beam and cross-sectional TEM techniques. Wear **207**, 152–162 (2011)

21. Wei, X., Hua, M., Xue, Z., Gao, Z., Li, J.: Evolution of friction-induced microstructure of SUS 304 meta-stable austenitic stainless steel and its influence on wear behavior. Wear **267**, 1386–1392 (2009)

22. Wang, X., Wei, X.C., Yang, X.R., Cheng, Z.B., Wang, W.R.: Atomic diffusion of gradient ultrafine structured surface layer produced by T10 steel rubbing against 20CrMnTi steel. Wear **304**, 118–125 (2013)

23. Kalin, M.: Influence of flash temperatures on the tribological behaviour in low-speed sliding: a review. Mater. Sci. Eng. A **374**, 390–397 (2004)

24. Qi, X.W., Jia, Z.N., Yang, Y.L., Fan, B.L.: Characterization and auto-restoration mechanism of nanoscale serpentine powder as lubricating oil additive under high temperature. Tribol. Int. **44**, 805–810 (2011)

25. Yang, Y.L., Ma, J., Qi, X.W., Meng, X.S.: Fabrication of nano serpentine–potassium acetate intercalation compound and its effect as additive on tribological properties of the fabric self-lubricating liner. Wear **318**, 202–211 (2014)

26. Lin, A., Takano, S., Hirono, T., Kanagawad, K.: Coseismic dehydration of serpentinite: evidence from high-velocity friction experiments. Chem. Geol. **344**, 50–62 (2013)

27. Kim, D.J., Chung, H.S.: Synthesis and characterization of ZSM-5 zeolite from serpentine. Appl. Clay Sci. **24**, 69–77 (2003)

28. Wang, X., Mao, D.D., Wei, X.C., Wang, W.R.: Cr atom diffusion in tribolayer T10 steel induced by dry sliding against 20CrMnTi steel. Appl. Surf. Sci. **270**, 145–149 (2013)

29. Yua, T.H., Torresa, R., Merinovb, B.V., Goddardb, W.A.: Elucidating challenges of reactions with correlated reactant and product binding energies on an example of oxygen reduction reaction. J. Mol. Catal. A Chem. **423**, 449–456 (2016)